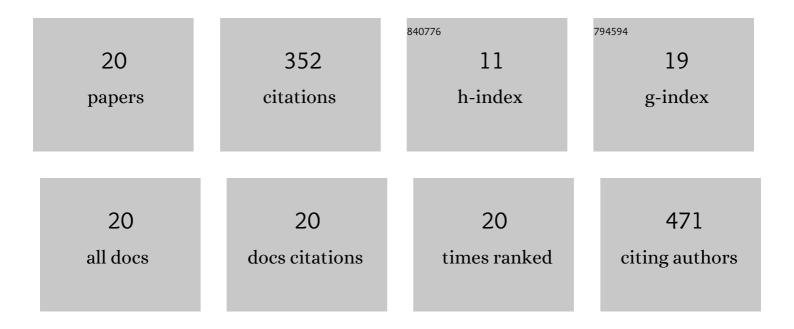


List of Publications by Year in descending order

Source: https://exaly.com/author-pdf/3316638/publications.pdf Version: 2024-02-01



VANCLI

#	Article	IF	CITATIONS
1	Boosting hydrogen evolution activity in alkaline media with dispersed ruthenium clusters in NiCo-layered double hydroxide. Electrochemistry Communications, 2019, 101, 23-27.	4.7	46
2	Growth of Fe 2 O 3 /SnO 2 nanobelt arrays on iron foil for efficient photocatalytic degradation of methylene blue. Chemical Physics Letters, 2017, 673, 1-6.	2.6	44
3	Hydrothermal preparation, growth mechanism and supercapacitive properties of WO ₃ nanorod arrays grown directly on a Cu substrate. CrystEngComm, 2016, 18, 3891-3904.	2.6	39
4	Simple synthesis of 1D, 2D and 3D WO3 nanostructures on stainless steel substrate for high-performance supercapacitors. Journal of Alloys and Compounds, 2019, 778, 603-611.	5.5	34
5	Defective carbon nanotube forest grown on stainless steel encapsulated in MnO2 nanosheets for supercapacitors. Electrochimica Acta, 2018, 278, 61-71.	5.2	29
6	Preparation and visible-light photocatalytic property of nanostructured Fe-doped TiO2 from titanium containing electric furnace molten slag. International Journal of Minerals, Metallurgy and Materials, 2013, 20, 1012-1020.	4.9	24
7	Tertiary structure of cactus-like WO 3 spheres self-assembled on Cu foil for supercapacitive electrode materials. Journal of Alloys and Compounds, 2017, 712, 345-354.	5.5	21
8	Influence of acid type and concentration on the synthesis of nanostructured titanium dioxide photocatalysts from titanium-bearing electric arc furnace molten slag. RSC Advances, 2015, 5, 13478-13487.	3.6	20
9	Fabrication of Mo-Doped WO3 Nanorod Arrays on FTO Substrate with Enhanced Electrochromic Properties. Materials, 2018, 11, 1627.	2.9	16
10	Selective Phase Transformation Behavior of Titanium-bearing Electric Furnace Molten Slag during the Molten NaOH Treatment Process. ISIJ International, 2015, 55, 134-141.	1.4	12
11	Synthesis of potassium hexatitanate whiskers with high thermal stability from Ti-bearing electric arc furnace molten slag. Ceramics International, 2016, 42, 11294-11302.	4.8	12
12	Insertion of Platinum Nanoparticles into MoS2 Nanoflakes for Enhanced Hydrogen Evolution Reaction. Materials, 2018, 11, 1520.	2.9	10
13	Mechanical and microstructural characterization of geopolymers synthesized from FCC waste catalyst and silica fume. Ceramics International, 2021, 47, 15186-15194.	4.8	9
14	Synthesis of TiO 2 visible light catalysts with controllable crystalline phase and morphology from Ti-bearing electric arc furnace molten slag. Journal of Environmental Sciences, 2016, 47, 14-22.	6.1	8
15	Polypyrrole Supported With Copper Nanoparticles Modified Alkali Anodized Steel Electrode for Probing of Glucose in Real Samples. IEEE Sensors Journal, 2018, 18, 5203-5212.	4.7	8
16	Optimizing the preheating temperature of hot rolled slab from the perspective of the oxidation kinetic. Journal of Materials Research and Technology, 2020, 9, 12501-12511.	5.8	8
17	Controllable synthesis of nanorod/nanodisk TiO2 from titanium-containing electric furnace molten slag. Rare Metals, 2015, 34, 267-275.	7.1	6
18	Preparation of stainless steel mesh-supported ZnO and graphene/ZnO nanorod arrays with high photocatalytic performance. Journal of Iron and Steel Research International, 2021, 28, 874-888.	2.8	3

#	Article	IF	CITATIONS
19	Favorable surface etching of NiRuFe(OH)x in neutral hydrogen evolution reaction. Catalysis Today, 2022, 400-401, 1-5.	4.4	2
20	Separation and comprehensive utilization of valuable elements in Ti-bearing electric arc furnace molten slag. Journal of Iron and Steel Research International, 2018, 25, 487-496.	2.8	1